

Oxygen atom transfer with organofunctionalized polyoxovanadium clusters: O-atom vacancy formation with tertiary phosphanes and deoxygenation of styrene oxide

Brittney E. Petel^a, Rachel L. Meyer^a, William W. Brennessel^a, Ellen M. Matson*^a

^a Department of Chemistry, University of Rochester, Rochester, NY 14627, USA.

Corresponding author email: matson@chem.rochester.edu

Supporting Information Table of Contents:

Figure S1. ^1H NMR spectra of optimization for 2-OPMe₃	S3
Figure S2. ^1H NMR spectra of 1 , 2-MeCN , and 2-OPMe₃	S3
Figure S3. ESI-MS (+)ve of 2-OPMe₃	S4
Figure S4. Infrared spectra of 2-OPMe₃	S4
Figure S5. Electronic absorption spectra of 2-OPMe₃	S5
Table S1. Crystallographic parameters of 2-OPMe₃	S6
Table S2. Bond valence sum calculations for 2-OPMe₃	S6
Figure S6. Molecular structure of 2-OPMe₃	S7
Table S3. Selected bond lengths of 2-OPMe₃	S7
Figure S7. ^1H NMR Spectrum of 2-OPMe₃ , 2-OPMe₂Ph , 2-OPMePh₂ , and 2-OPPh₃	S8
Figure S8. ESI-MS (+)ve of 2-OPMe₂Ph	S8
Figure S9. ESI-MS (+)ve of 2-OPMePh₂	S9
Figure S10. ESI-MS (+)ve of 2-OPPh₃	S9
Table S4. Crystallographic parameters of 2-OPMe₂Ph , 2-OPMePh₂ , and 2-OPPh₃	S10
Table S5. Selected bond lengths and angles of 2-OPMe₂Ph , 2-OPMePh₂ , and 2-OPPh₃	S10
Table S6. Bond valence sum calculations for 2-OPMe₂Ph , 2-OPMePh₂ , and 2-OPPh₃	S11
Table S7. Bond vibrations of 2-OPMe₃ , 2-OPMe₂Ph , 2-OPMePh₂ , and 2-OPPh₃	S11
Table S8. Relationship between nucleophilicity, cone angle, and reaction time	S12
Figure S11. ^1H NMR Spectrum of $\text{V}_6\text{O}_5(\text{OMe})_{12}(\text{OPMe}_2\text{Ph})_2$	S12
Figure S12. ESI-MS (+)ve of $\text{V}_6\text{O}_5(\text{OMe})_{12}(\text{OPMe}_2\text{Ph})_2$	S13
Figure S13. ^1H NMR Spectrum of 4-OPMe₃	S13
Figure S14. Infrared spectra of 3 , 4-MeCN , 4-OPMe₃ , and 4-OPMe₂Ph	S14
Table S9. Bond vibrations of 4-MeCN , 4-OPMe₃ , and 4-OPMe₂Ph	S14
Figure S15. Electronic absorption spectra of 3 , 4-MeCN , 4-OPMe₃ , and 4-OPMe₂Ph	S15
Figure S16. ^1H NMR spectra of 4-MeCN and 4-OPMe₂Ph in CD_3CN	S15
Figure S17. ^1H NMR spectrum of 4-OPMe₂Ph in CD_2Cl_2	S16
Figure S18. Molecular structure of 4-OPMe₂Ph	S16
Table S10. Crystallographic parameters of 4-OPMe₂Ph	S17
Figure S19. ^1H NMR spectra of attempted synthesis of 4-OPMePh₂	S18
Figure S20. ^1H NMR spectra of attempted synthesis of 4-OPPh₃	S18
Figure S21. ^1H NMR spectra of $[\text{V}_6\text{O}_7(\text{OPr})_{12}]^0 + \text{PR}_3$	S19
Figure S22. Diamagnetic ^1H NMR spectra of 2-OPMe₃ + styrene oxide	S20
Figure S23. Paramagnetic ^1H NMR spectra of 2-OPMe₃ + styrene oxide	S20
Figure S24. Paramagnetic ^1H NMR spectra of 2-OPMe₃ + excess styrene oxide	S21
Figure S25. Paramagnetic ^1H NMR spectra of 4-OPMe₃ + styrene oxide	S22
Figure S26. Diamagnetic ^1H NMR spectra of 4-OPMe₃ + styrene oxide	S22
References	S23

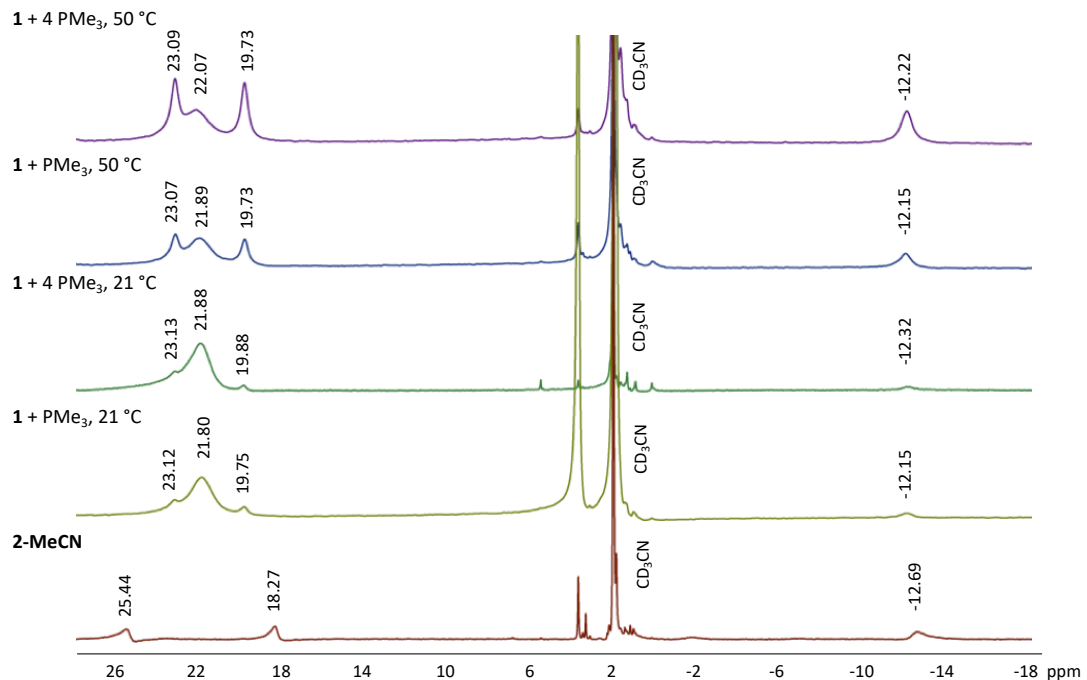


Figure S1. ¹H NMR spectra of the reaction mixtures of [V₆O₇(OMe)₁₂]⁰ (**1**) and PMe₃ (1 or 4 equiv) after stirring at 21 or 50 °C for 24 hours in THF (see labels for reaction details). All spectra were collected in CD₃CN at 21 °C.

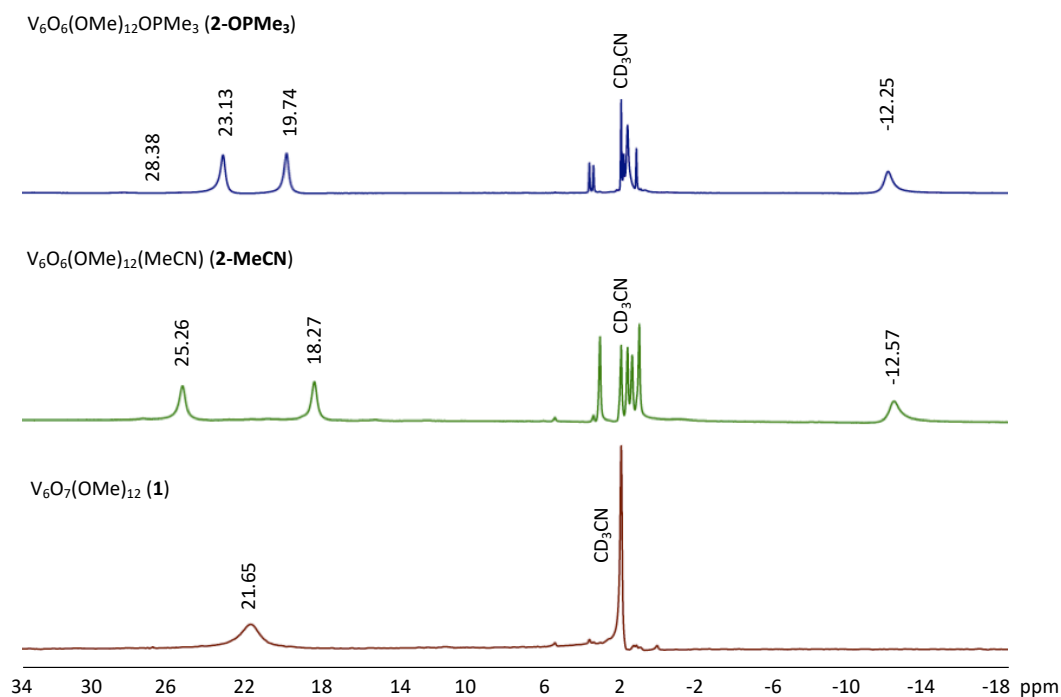


Figure S2. ¹H NMR spectrum of **1** (bottom, red), **2-MeCN** (middle, green), and **2-OPMe₃** (top, blue) in CD₃CN at 21 °C.

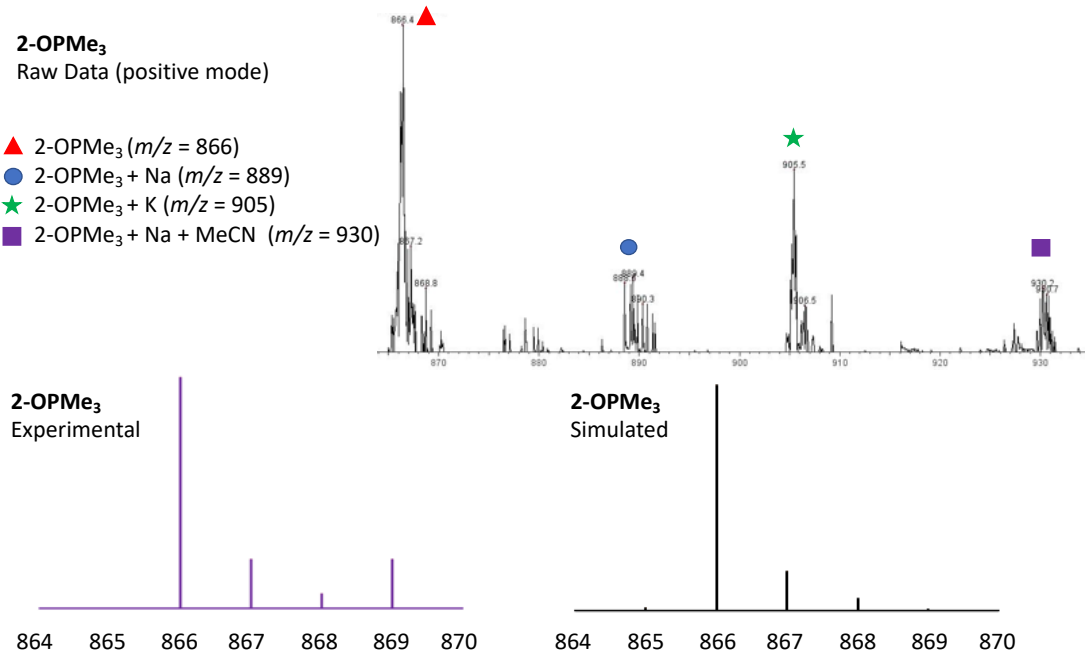


Figure S3. ESI-MS (+)ve of **2-OPMe₃** ($m/z = 866$).

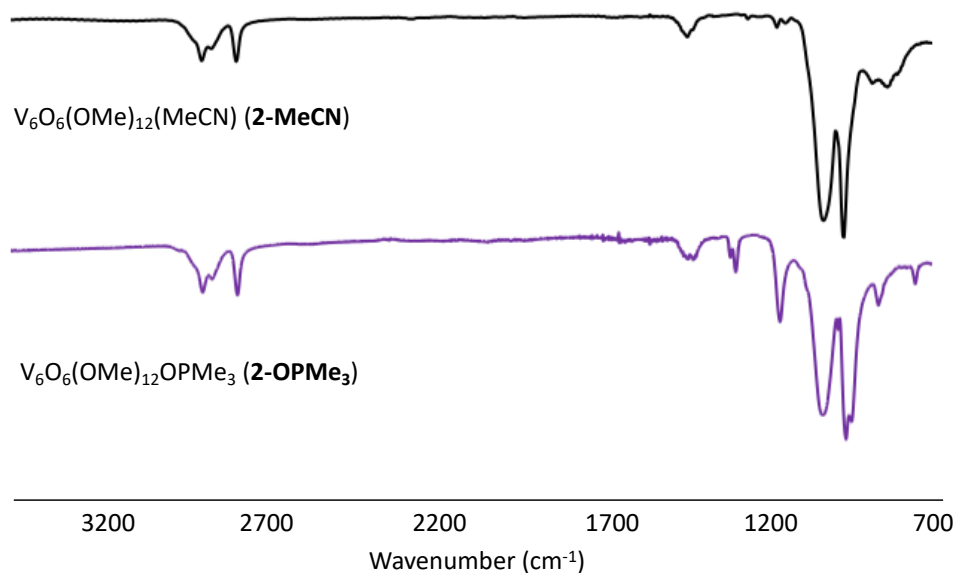


Figure S4. Infrared absorption spectra of **2-MeCN** (top, black), and **2-OPMe₃** (bottom, purple). See Table S7 for bond vibrations.

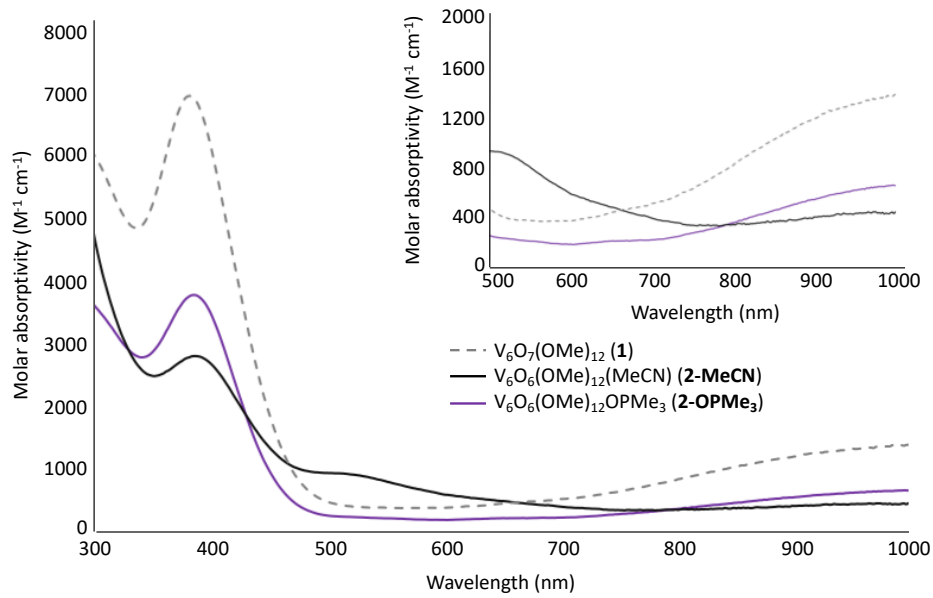


Figure S5. Electronic absorption spectra of complexes **1** (grey dashed), **2-MeCN** (black), and **2-OPMe₃** (purple) collected in acetonitrile at 21 °C.

Table S1. Crystallographic Parameters of **2-OPMe₃** (CCDC: 191251)

Empirical formula	C ₁₅ H ₄₅ PO ₁₉ V ₆		
Formula weight	866.12		
Temperature	192.99(10) K		
Wavelength	1.54184 Å		
Crystal system	Monoclinic		
Space group	P 2 ₁ /c		
Unit cell dimensions	a = 20.7527(3) Å b = 20.6175(3) Å c = 17.6285(3) Å	$\alpha = 90^\circ$ $\beta = 106.417(2)^\circ$ $\gamma = 90^\circ$	
Volume	7235.2(2) Å ³		
Z	8		
Reflections collected	62308		
Independent reflections	15129		
Goodness-of-fit on F ²	1.048		
Final R indices [I>2sigma(I)]	R1 = 0.0967, wR2 = 0.2638		

Table S2. Bond valence sum calculations for the crystallographically independent vanadium ions in **2-OPMe₃** based on X-ray crystallographic data collected at 193 K. Table reflects the results of BVS calculations using V-O bond valence parameters (r_0) for different oxidation states of vanadium.

2-OPMe₃	V1	V2	V3	V4	V5	V6
V(III)	3.102	4.005	3.970	4.033	4.076	4.471
V(IV)	3.176	4.100	4.065	4.129	4.173	4.577
V(V)	3.414	4.370	4.333	4.401	4.446	4.872

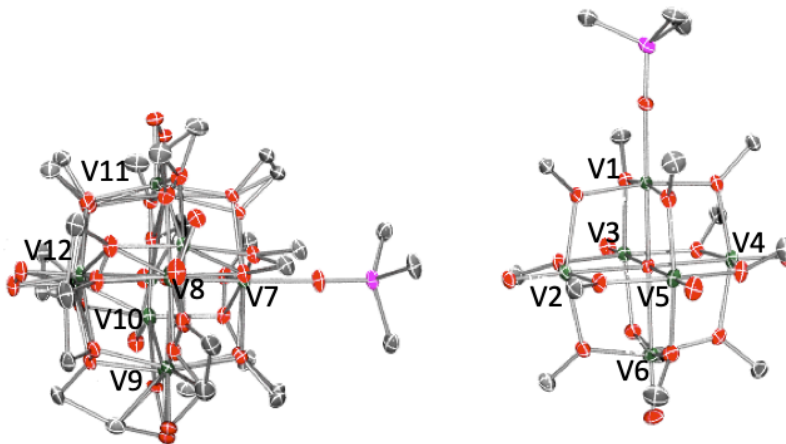


Figure S6. Molecular structures of both independent molecules in the asymmetric unit of **2-OPMe₃** shown with 10% probability ellipsoids. Hydrogen atoms removed for clarity. Highly disordered structure (left, atoms V7-V12) is disordered over two positions due to adjacency with its symmetry equivalents. Bond metrics of **2-OPMe₃** obtained from the molecule without disorder (right, atoms V1-V6).

Table S3. Selected bond lengths and angles of **2-OPMe₃** and comparison to previously reported mono- and di-vacant complexes.

Bond Distances and Angles	V ₆ O ₇ (OMe) ₁₂ (1)	V ₆ O ₆ (OMe) ₁₂ OPMe ₃ (2-OPMe₃)	V ₆ O ₆ (OMe) ₁₂ OTf	V ₆ O ₅ (OMe) ₁₂ (MeCN) ₂
Reference	Hartl, 2005 ¹	This work	Matson, 2018 ²	Matson, 2019 ³
V1-O1	--	2.026(5) Å	2.052(8) Å	--
O=P	--	1.467(6) Å	--	--
V1-O _c	2.25 Å	2.120(5) Å	2.079(4) Å	2.0666(17) Å 2.0760(17) Å
V=O _t (avg.)	1.60 Å	1.592 Å	1.585 Å	1.605 Å
V1-O _b -V _n (avg.)	--	~105°	~105°	~105°

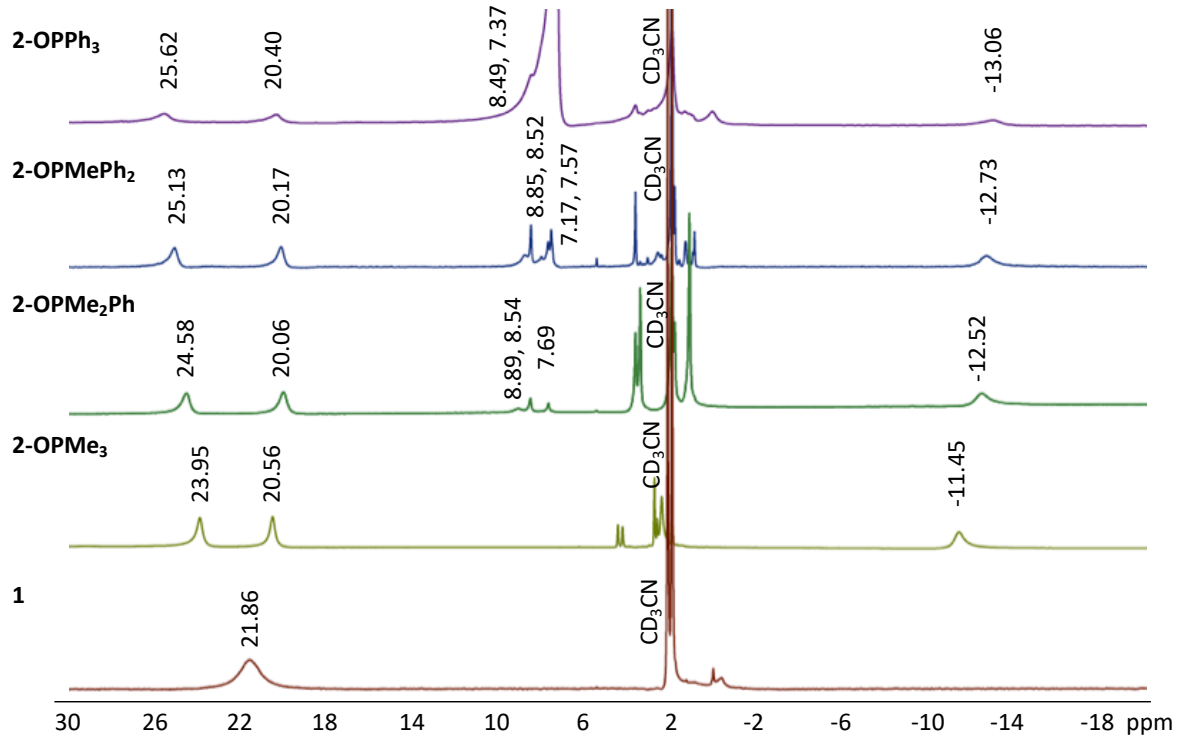


Figure S7. ^1H NMR spectrum of **1** (red), **2-OPMe₃** (yellow), **2-OPMe₂Ph** (green), **2-OPMePh₂** (blue) and **2-OPPh₃** (purple) in CD_3CN at 21 °C.

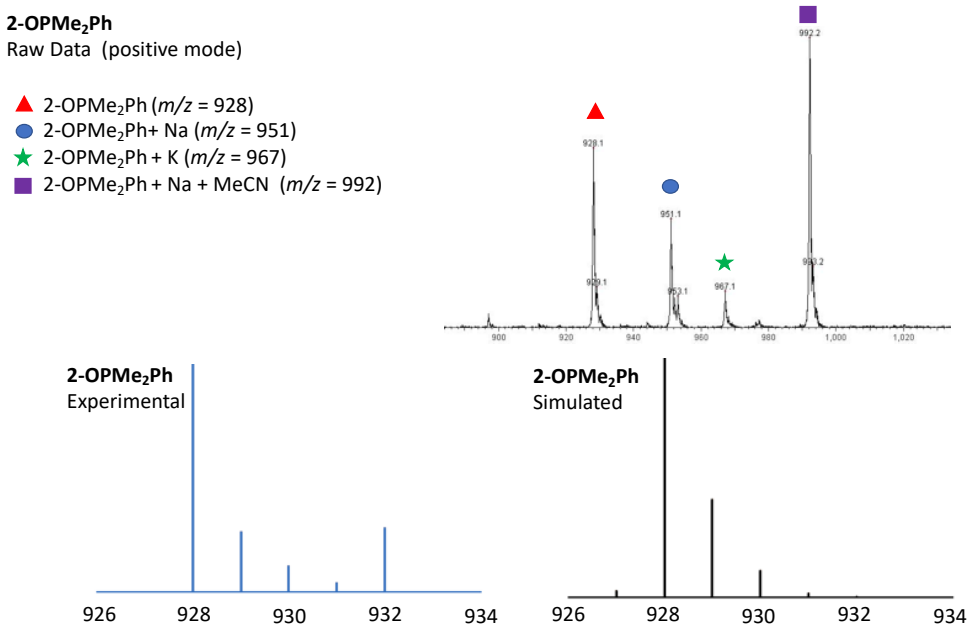


Figure S8. ESI-MS (+)ve of **2-OPMe₂Ph** (m/z = 928).

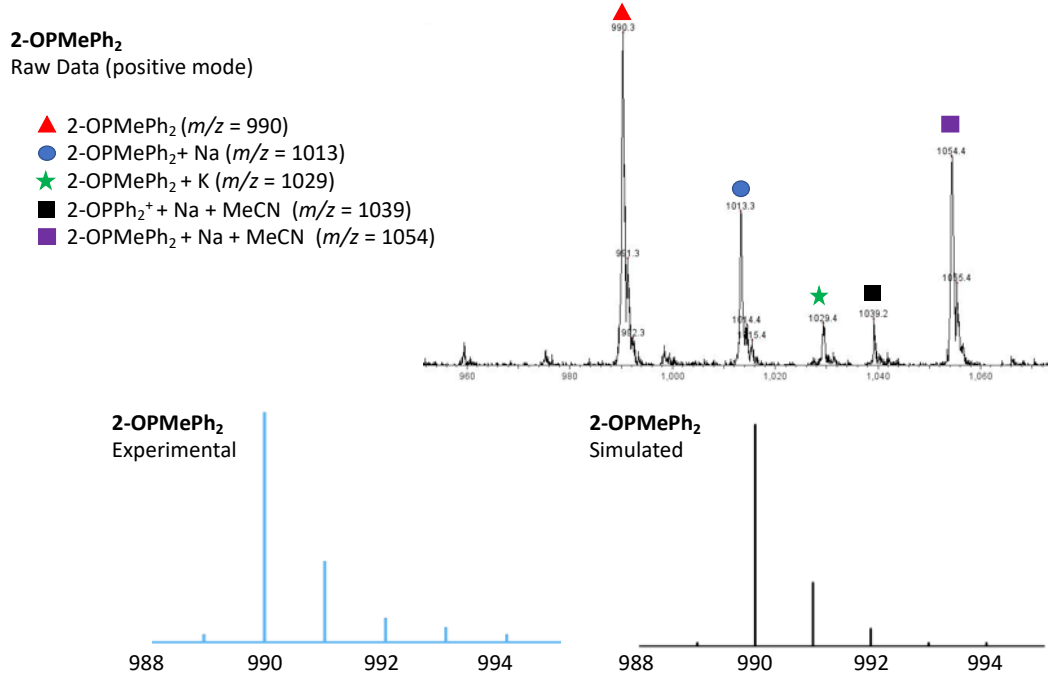


Figure S9. ESI-MS (+)ve of 2-OPMePh₂ ($m/z = 990$).

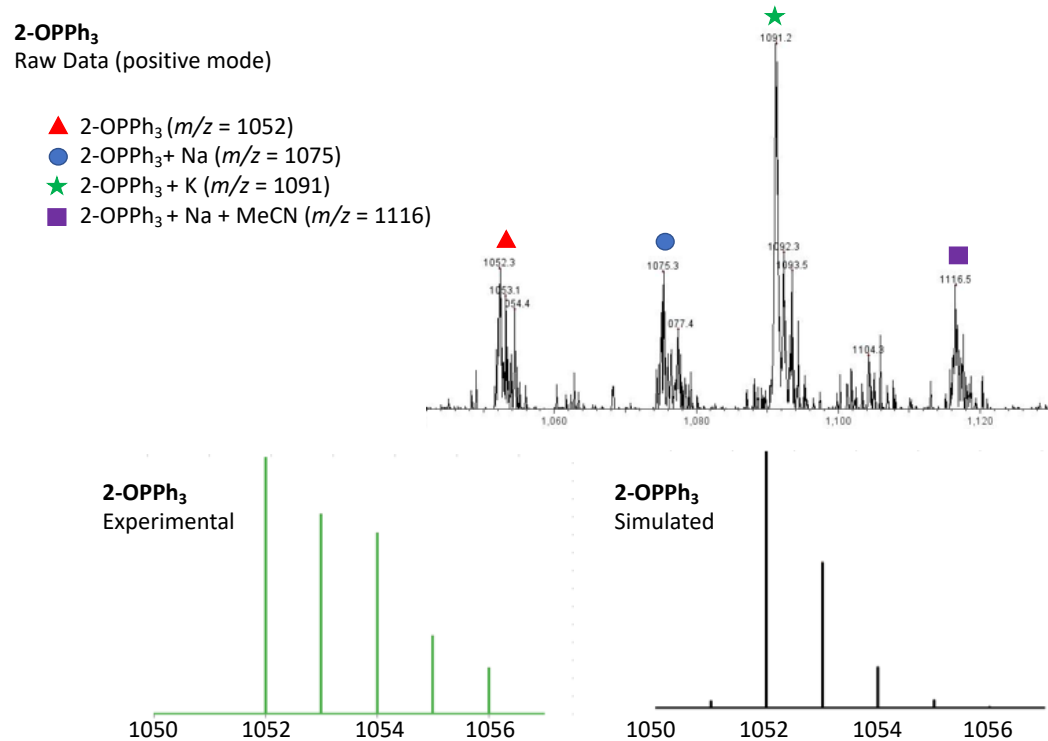


Figure S10. ESI-MS (+)ve of 2-OPPh₃ ($m/z = 1052$).

Table S4. Crystallographic Parameters of **2-OPMe₂Ph**, **2-OPMePh₂**, and **2-OPPh₃** (CCDC: 1914252 – 1914254).

Molecule	2-OPMe₂Ph	2-OPMePh₂	2-OPPh₃
Empirical formula	C ₂₀ H ₄₇ PO ₁₉ V ₆	C ₂₅ H ₄₉ PO ₁₉ V ₆	C ₃₀ H ₅₁ PO ₁₉ V ₆
Formula weight	928.18	990.25	1052.31
Temperature	100.00(10) K	100.0(4) K	100.0(5) K
Wavelength	1.54184 Å	1.54184 Å	1.54184 Å
Crystal system	Monoclinic	Monoclinic	Orthorhombic
Space group	C 2/c	P2 ₁	P2 ₁ 2 ₁ 2 ₁
Unit cell dimensions	a = 33.3410(3) Å b = 10.76690(10) Å c = 20.2152(2) Å α = 90° β = 92.6080(10)° γ = 90°	a = 11.0627(8) Å b = 10.8304(7) Å c = 16.9545(12) Å α = 90° β = 108.004(8)° γ = 90°	a = 13.72880(10) Å b = 16.00950(10) Å c = 18.8692(2) Å α = 90° β = 90° γ = 90°
Volume	7249.43(12) Å ³	1.931.9(2) Å ³	4147.28(6) Å ³
Z	8	2	4
Reflections collected	34073	27440	38388
Independent reflections	7553	7696	8699
Goodness-of-fit on F2	1.079	1.093	1.090
Final R indices [I>2sigma(I)]	R1 = 0.0414 wR2 = 0.1165	R1 = 0.1213 wR2 = 0.2832	R1 = 0.0395 wR2 = 0.1074

Table S5. Selected bond lengths and angles of **2-OPMe₂Ph**, **2-OPMePh₂**, and **2-OPPh₃**.

Bond Distances and Angles	2-OPMe₂Ph	2-OPMePh₂	2-OPPh₃
V1-O1	2.0403(19) Å	2.052(14) Å	2.049(3) Å
O=P	1.5032(19) Å	1.487(15) Å	1.506(3) Å
V1-O _c	2.0982(17) Å	2.112(14) Å	2.117(3) Å
V=O _t (avg.)	1.5998 Å	1.6002 Å	1.598 Å
V1-O _b -V _n (avg.)	~105°	~104°	~104°

Table S6. Bond valence sum calculations for the crystallographically independent vanadium ions in **2-OPMe₂Ph**, **2-OPMePh₂**, and **2-OPPh₃** based on X-ray crystallographic data collected at 100 K. Table reflects the results of BVS calculations using V-O bond valence parameters (r_0) for different oxidation states of vanadium.

2-OPMe₂Ph	V1	V2	V3	V4	V5	V6
V(III)	3.097	3.886	4.483	3.9955	3.894	3.950
V(IV)	3.171	3.979	4.590	4.049	3.986	4.044
V(V)	3.409	4.243	4.886	4.317	4.250	4.31

2-OPMePh₂	V1	V2	V3	V4	V5	V6
V(III)	3.004	3.909	3.821	3.899	4.049	4.445
V(IV)	3.076	4.002	3.912	3.992	4.146	4.551
V(V)	3.308	4.268	4.174	4.257	4.416	4.845

2-OPPh₃	V1	V2	V3	V4	V5	V6
V(III)	3.097	4.110	4.500	3.955	3.894	3.953
V(IV)	3.171	4.208	4.607	4.049	3.986	4.048
V(V)	3.409	4.487	4.904	4.317	4.250	4.315

Table S7. Bond vibrations (cm⁻¹) of **2-OPMe₃**, **2-OPMe₂Ph**, **2-OPMePh₂**, and **2-OPPh₃**.

	2-OPMe₃	2-OPMe₂Ph	2-OPMePh₂	2-OPPh₃
V=O	962 cm ⁻¹	962 cm ⁻¹	964 cm ⁻¹	966 cm ⁻¹
O-CH ₃	1032 cm ⁻¹	1036 cm ⁻¹	1036 cm ⁻¹	1040 cm ⁻¹
P=O	1163 cm ⁻¹	1159 cm ⁻¹	1159 cm ⁻¹	1157 cm ⁻¹

Table S8. Relationship between phosphine nucleophilicity (pK_a or an electronic parameter derived from $\nu(\text{CO})$ of a nickel compound), cone angle, and reaction time for formation of all (OPR_3) -bound clusters.

	PMe₃	PMe₂Ph	PMePh₂	PPh₃
pK_a^4	8.65	6.50	4.59	2.73
Electronic parameter ⁵	2064.1	2065.3	2067.0	2068.9
Tolman Cone Angle ⁵	118	122	136	145
Reaction time with 1	19 hrs	7 hrs	28 hrs	15 days

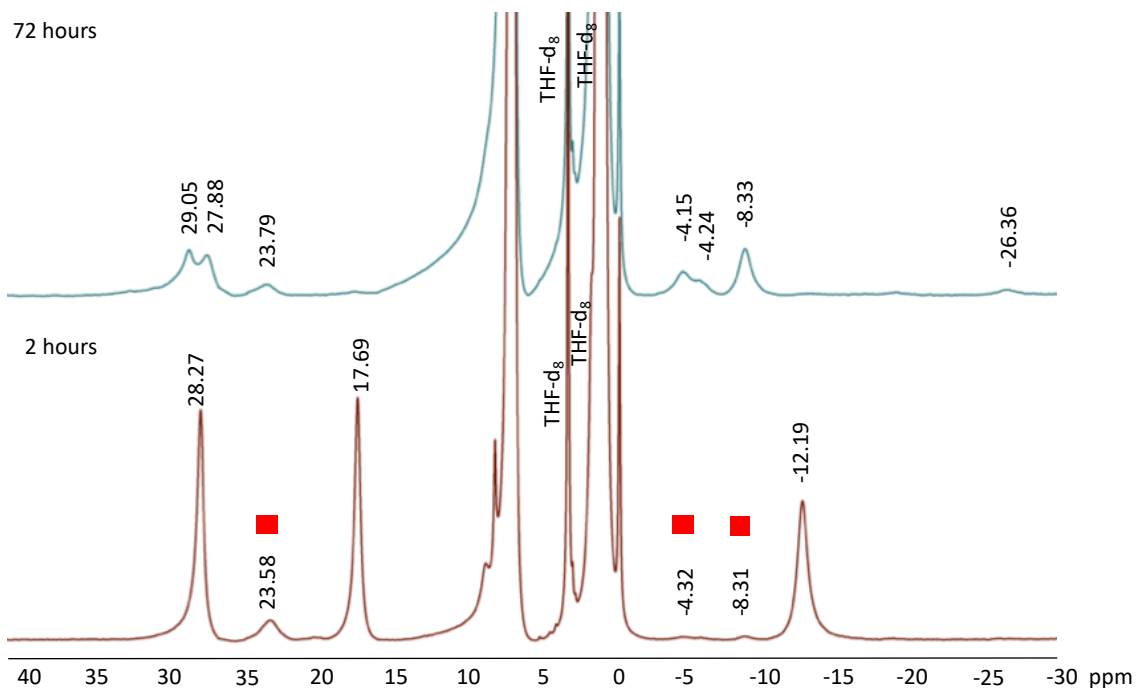


Figure S11. ¹H NMR spectrum of a J-young scale reaction of addition of 4 equiv PMe₂Ph to complex **1** in THF-d₈ at 70 °C. The 2 h time point (bottom, red) shows formation of the mono-vacant product, **2-OPMe₂Ph** and the over-reduced molecule, V₆O₅(OMe)₁₂(OPMe₂Ph)₂ (denoted by red squares). Allowing the reaction to stir for 72 h (top, blue) results in complete conversion to the (OPMe₂Ph)₂-bound molecule, confirmed by ESI-MS (Figure S12).

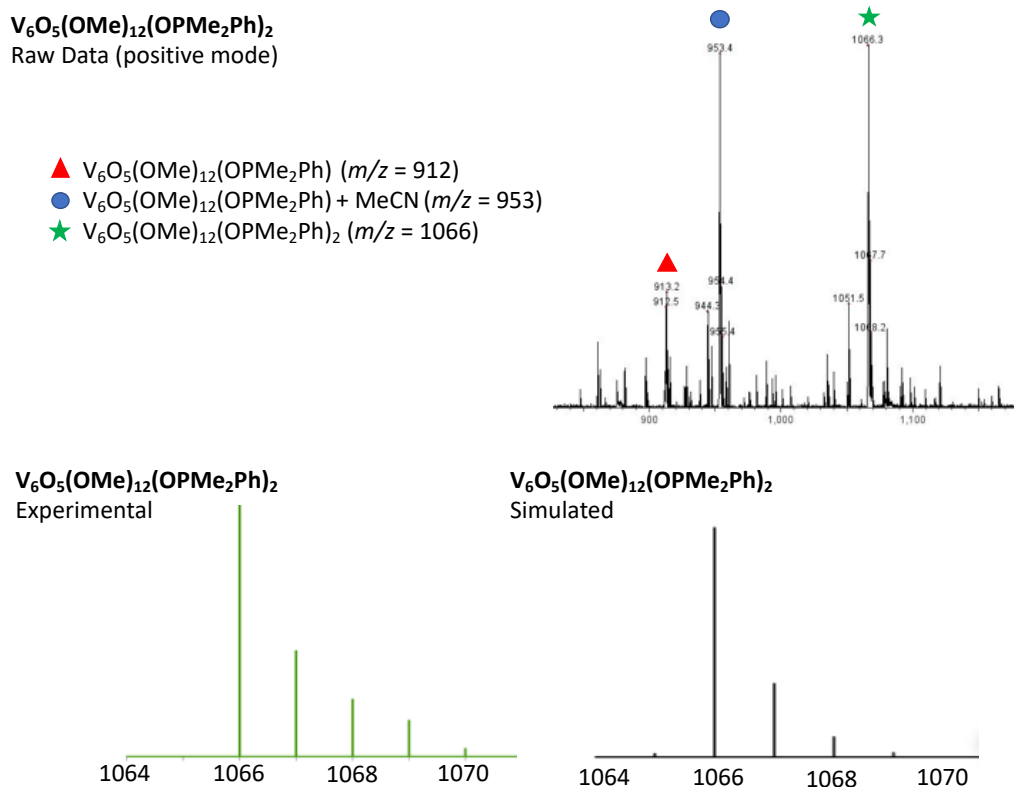


Figure S12. ESI-MS (+)ve of the (OPMe_2Ph)₂-bound molecule, $\text{V}_6\text{O}_5(\text{OMe})_{12}(\text{OPMe}_2\text{Ph})_2$ ($m/z = 1066$).

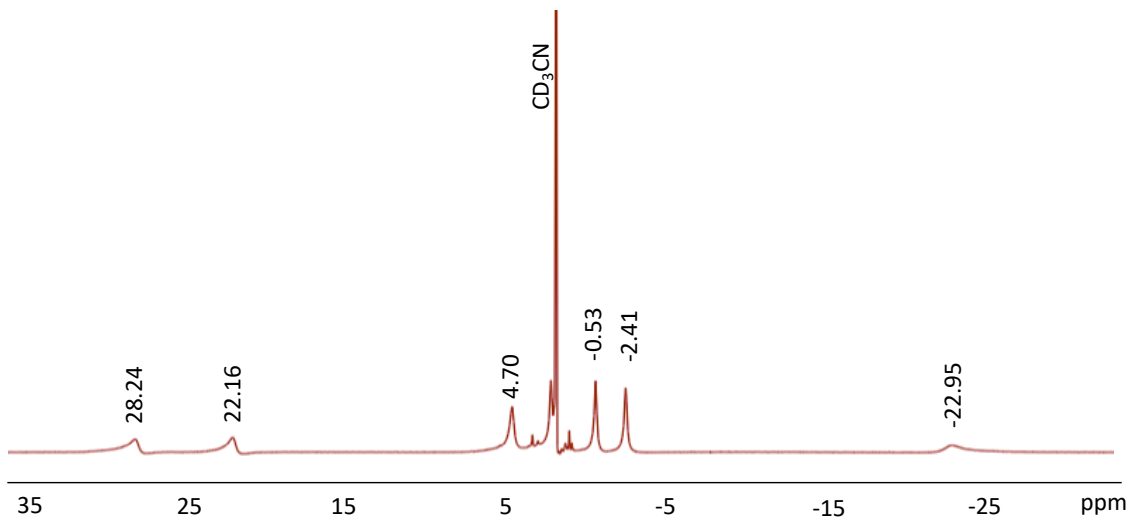


Figure S13. ^1H NMR spectrum of **4-OPMe₃** in CD_3CN at 21 °C.

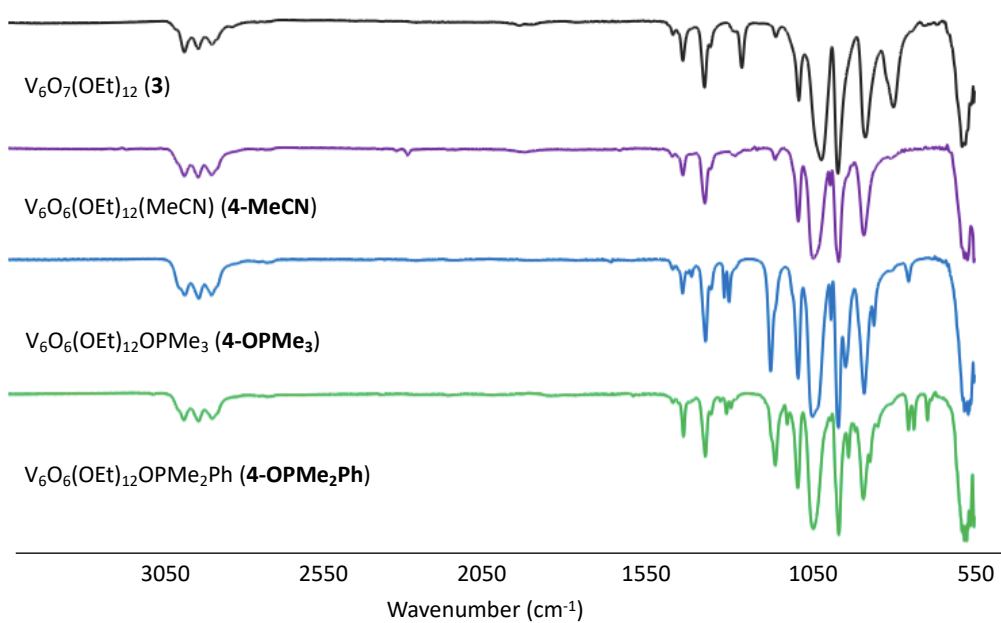


Figure S14. Infrared absorption spectra of **3** (black), **4-MeCN** (purple), **4-OPMe₃** (blue), and **4-OPMe₂Ph** (green). See Table S9 for bond vibrations.

Table S9. Bond vibrations (cm⁻¹) of **4-MeCN**, **4-OPMe₃**, and **4-OPMe₂Ph**.

	4-MeCN	4-OPMe₃	4-OPMe₂Ph
V=O	964 cm ⁻¹	964 cm ⁻¹	964 cm ⁻¹
O-CH ₃	1040 cm ⁻¹	1042 cm ⁻¹	1040 cm ⁻¹
P=O	---	1171 cm ⁻¹	1157 cm ⁻¹

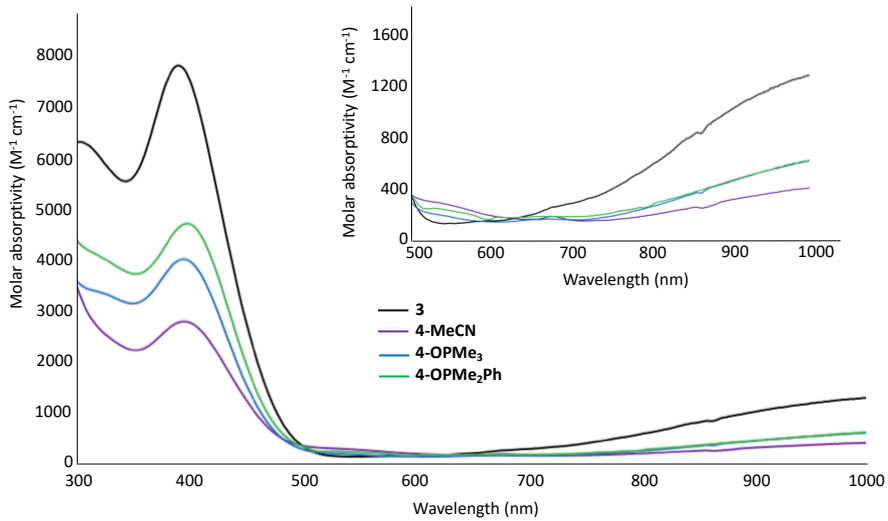


Figure S15. Electronic absorption spectra of complexes **3** (black), **4-MeCN** (purple), **4-OPMe₃** (blue), and **4-OPMe₂Ph** (green) collected in dichloromethane at 21 °C.

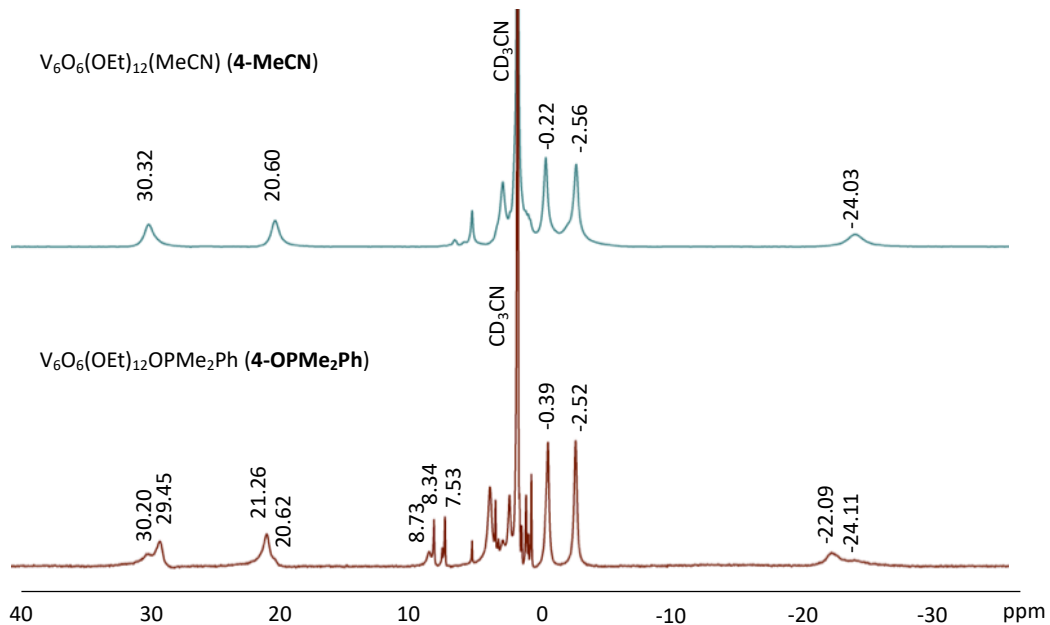


Figure S16. ¹H NMR spectra of complexes **4-OPMe₂Ph** (bottom, red), and **4-MeCN** (top, blue) collected in CD₃CN at 21 °C.

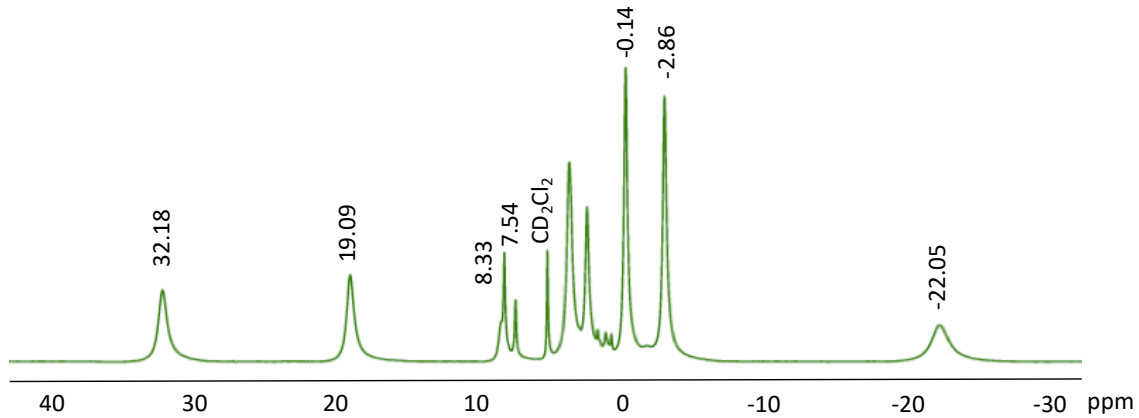


Figure S17. ^1H NMR spectra of **4-OPMe₂Ph** in CD_2Cl_2 at 21 °C.

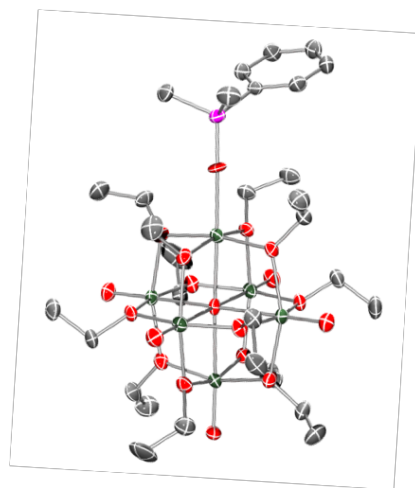


Figure S18. Molecular structure of **4-OPMe₂Ph** shown with 50% probability ellipsoids. Hydrogen atoms removed for clarity. The molecules are arranged in head-to-tail chains (the head being the phosphine oxide ligand and the tail being the vanadyl group on the opposite side of the molecule) that are disordered with chains directed in the opposite direction. Due to the disorder and the restraints required to model it, bond lengths and angles cannot be obtained.

Table S10. Crystallographic Parameters of **4-OPMe₂Ph** (CCDC: 1914250).

Empirical formula	C ₃₂ H ₇₁ PO ₁₉ V ₆		
Formula weight	1096.49		
Temperature	100.0(3) K		
Wavelength	1.54184 Å		
Crystal system	Monoclinic		
Space group	<i>Cc</i>		
Unit cell dimensions	a = 20.7441(3) Å b = 10.74980(16) Å c = 21.6524(3) Å	$\alpha = 90^\circ$ $\beta = 101.7536(14)^\circ$ $\gamma = 90^\circ$	
Volume	4727.14(12) Å ³		
Z	4		
Reflections collected	45966		
Independent reflections	9141		
Goodness-of-fit on F ²	1.055		
Final R indices [I>2sigma(I)]	R1 = 0.0568, wR2 = 0.1553		

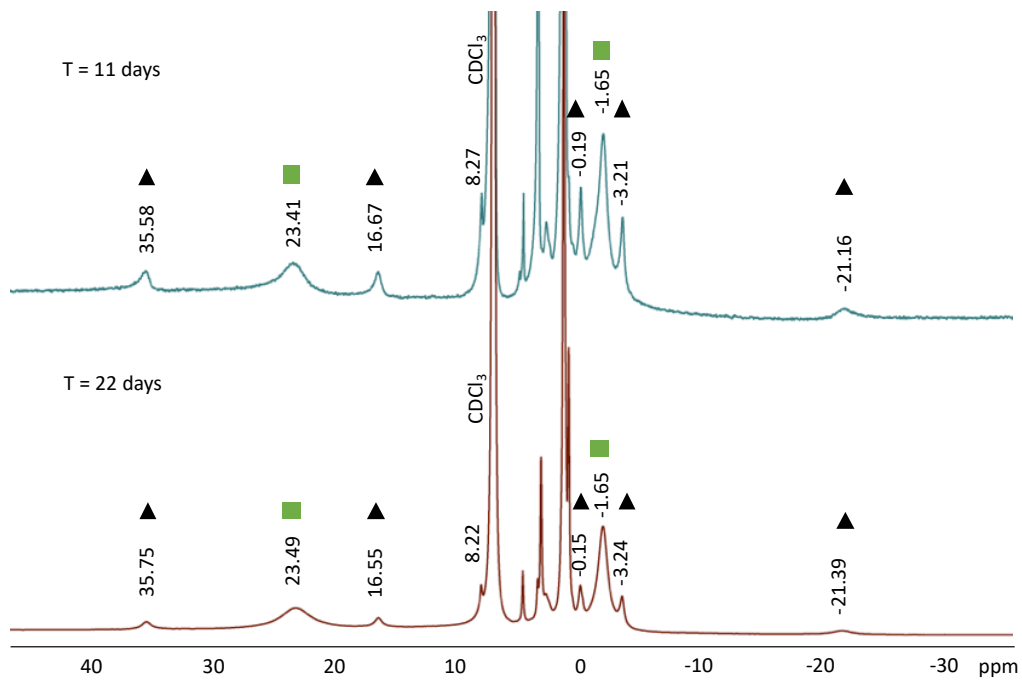


Figure S19. ^1H NMR spectra of attempted synthesis of **4-OPMePh₂** (black triangles) collected in CDCl_3 at 21 °C. Time points following addition of PMePh_2 (4 equiv) to **3** (green squares) after stirring at 70 °C for over two weeks in a 15 mL pressure vessel show incomplete conversion to **3**.

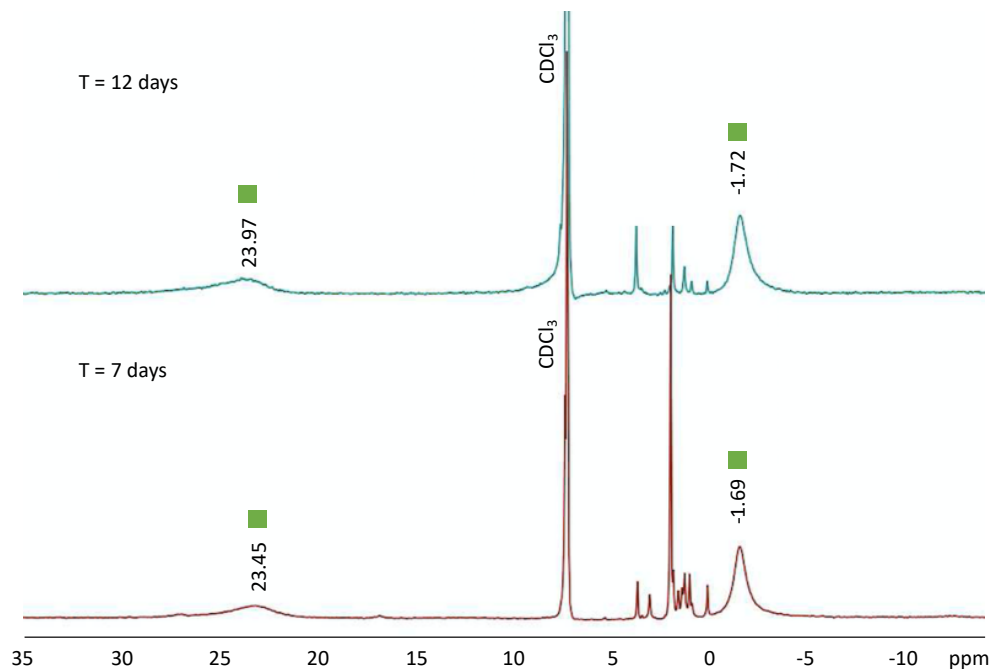


Figure S20. ^1H NMR spectra of attempted synthesis of **4-OPPh₃** collected in CDCl_3 at 21 °C. Time points following addition of PPh_3 (4 equiv) to **3** after stirring at 70 °C for over a week in a 15 mL pressure vessel show no conversion of **3** (green squares) after 12 days.

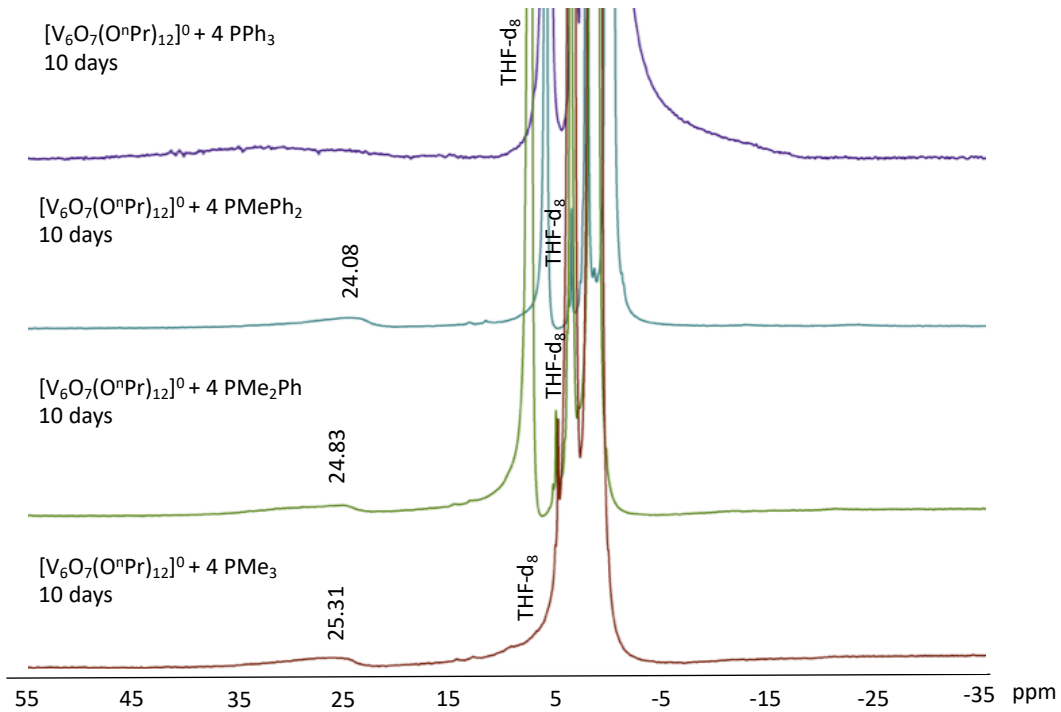


Figure S21. ^1H NMR spectra of a mixture of the propoxide-bridged cluster, $[\text{V}_6\text{O}_7(\text{O}^n\text{Pr})_{12}]^0$, and a series of phosphanes (4 equiv). Spectra were collected in THF-d_8 at 21 °C. All mixtures were heated to 70 °C for 10 days in a J-young tube. Time points show no conversion of $[\text{V}_6\text{O}_7(\text{O}^n\text{Pr})_{12}]^0$.

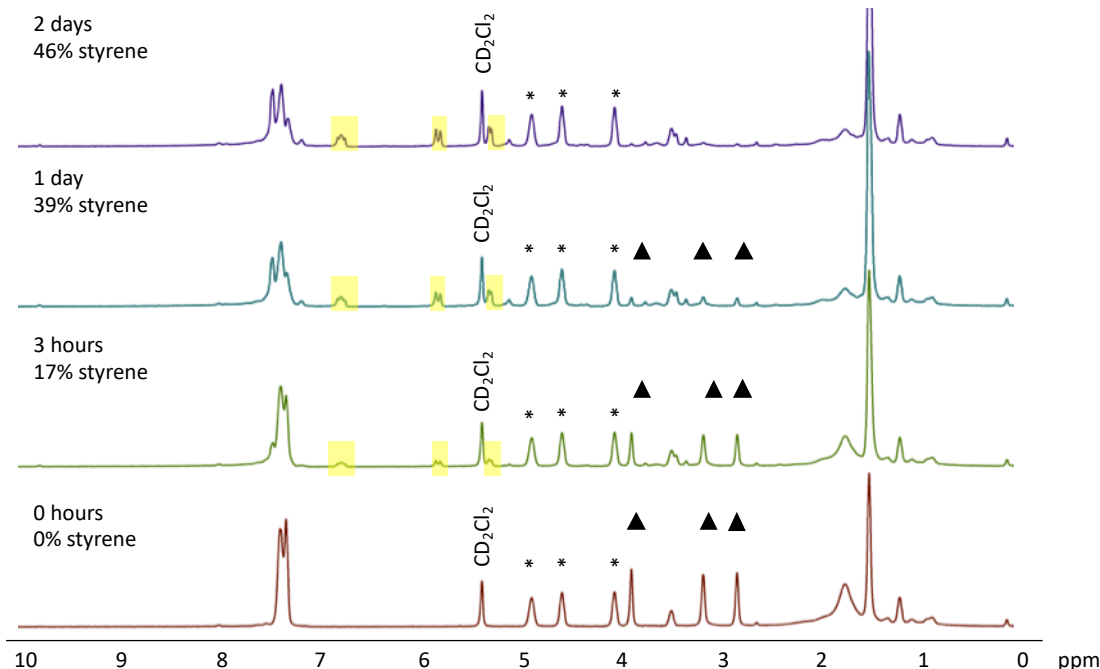


Figure S22. Representative ^1H NMR spectra of the diamagnetic region of a crude reaction mixture of **2-OPMe₃** and styrene oxide (1 equiv) at 70 °C in CD_2Cl_2 . Time points reveal loss of styrene oxide (black triangles) and growth of styrene (yellow highlight). Propylene carbonate (denoted by ‘*’) was used as a ^1H NMR internal standard.

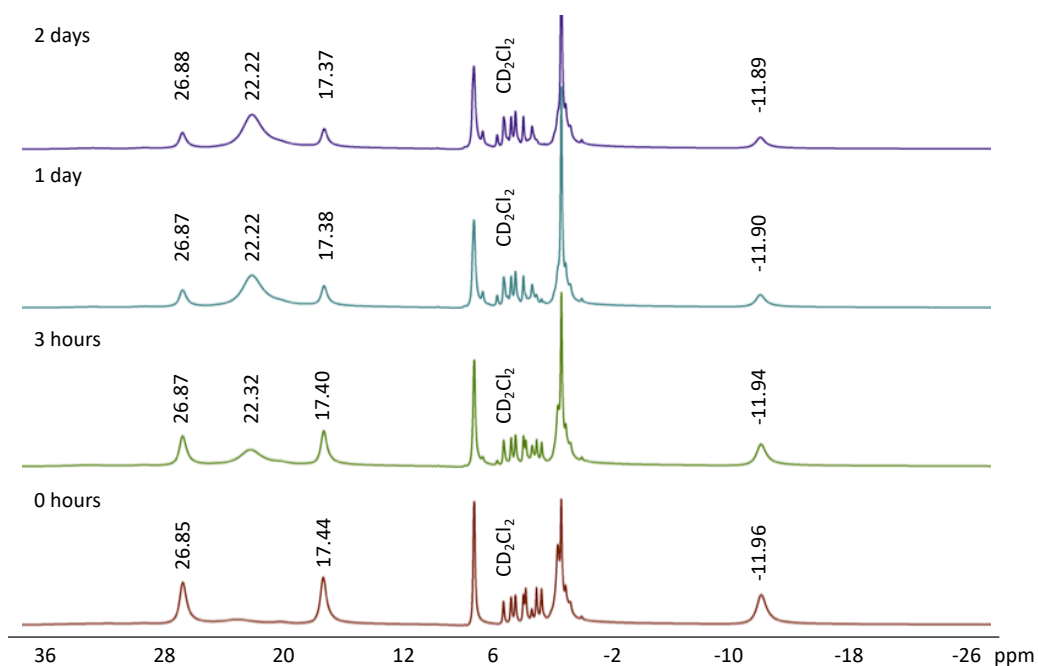


Figure S23. ^1H NMR spectra highlighting the paramagnetic region of the crude reaction mixture of **2-OPMe₃** and styrene oxide (1 equiv) at 70 °C in CD_2Cl_2 . Time points show growth of a resonance corresponding to complex **1** (22.2 ppm).

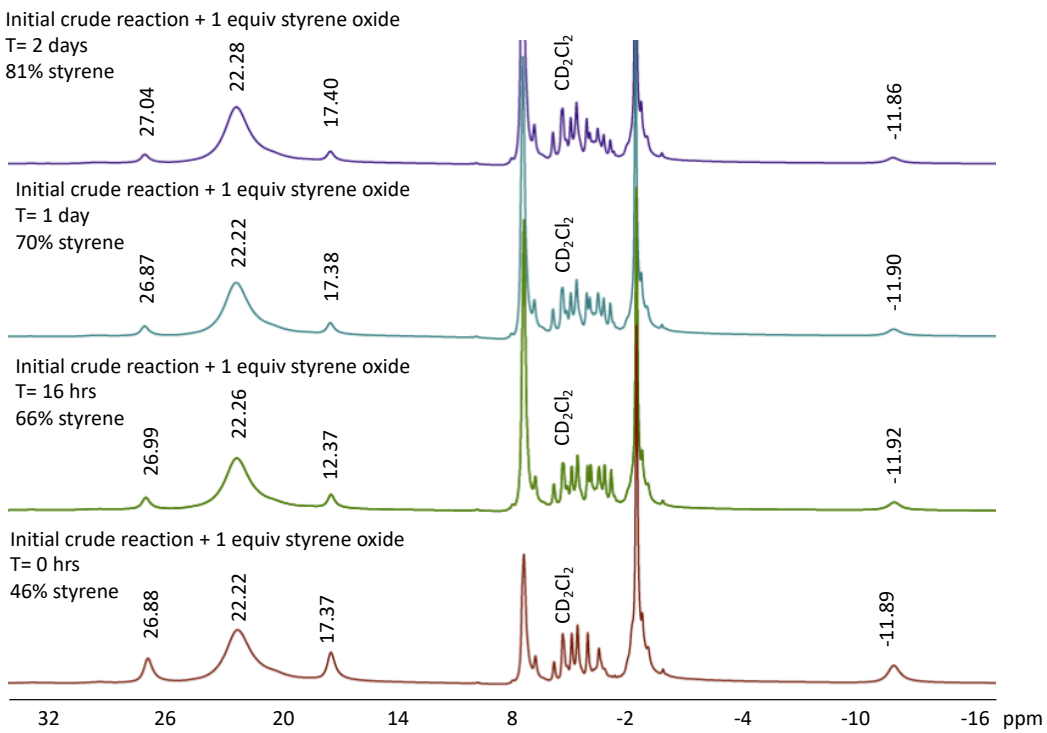


Figure S24. ^1H NMR spectra of the addition of *excess* styrene oxide (1 equiv) to the crude reaction mixture of **2-OPMe₃** and styrene oxide after 2 days at 70 °C (CD_2Cl_2 , see Figure S23 for initial time points of this reaction). Time points show further oxidation of **2-OPMe₃** to **3** (23.4, -1.60 ppm) after an additional 2 days. Yields reported are total yields from both experiments.

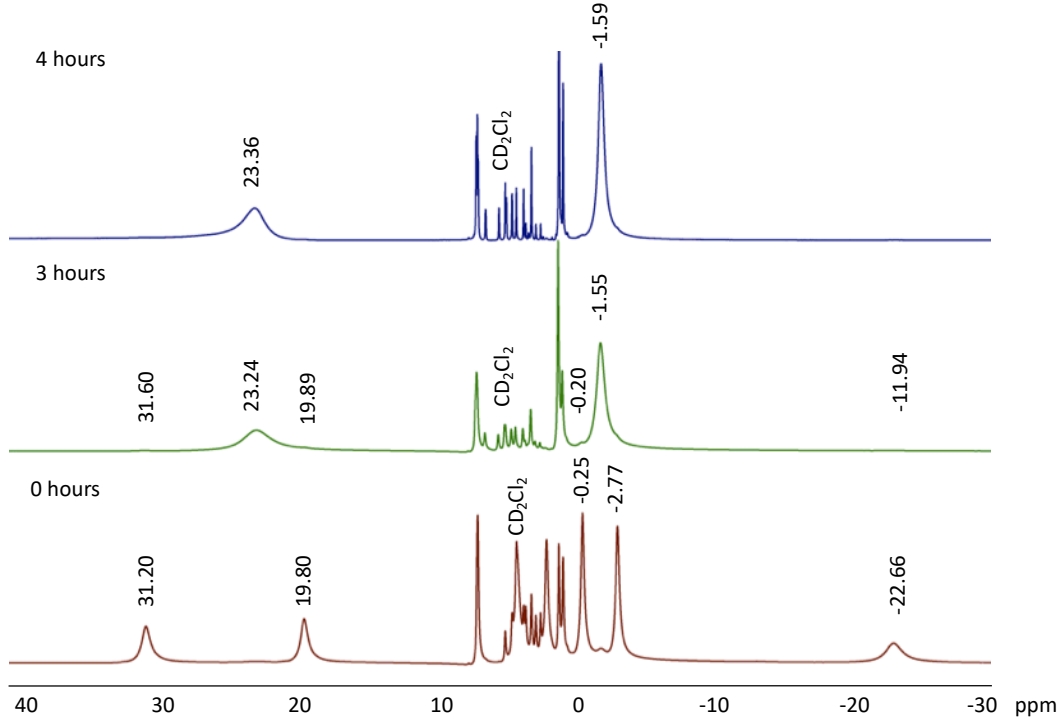


Figure S25. ^1H NMR spectra of paramagnetic region of the crude reaction mixture of **4-OPMe₃** and styrene oxide (1 equiv) at 70 °C in CD_2Cl_2 . Time points show complete conversion of **4-OPMe₃** to **3** (23.4, -1.60 ppm) after 4 hours.

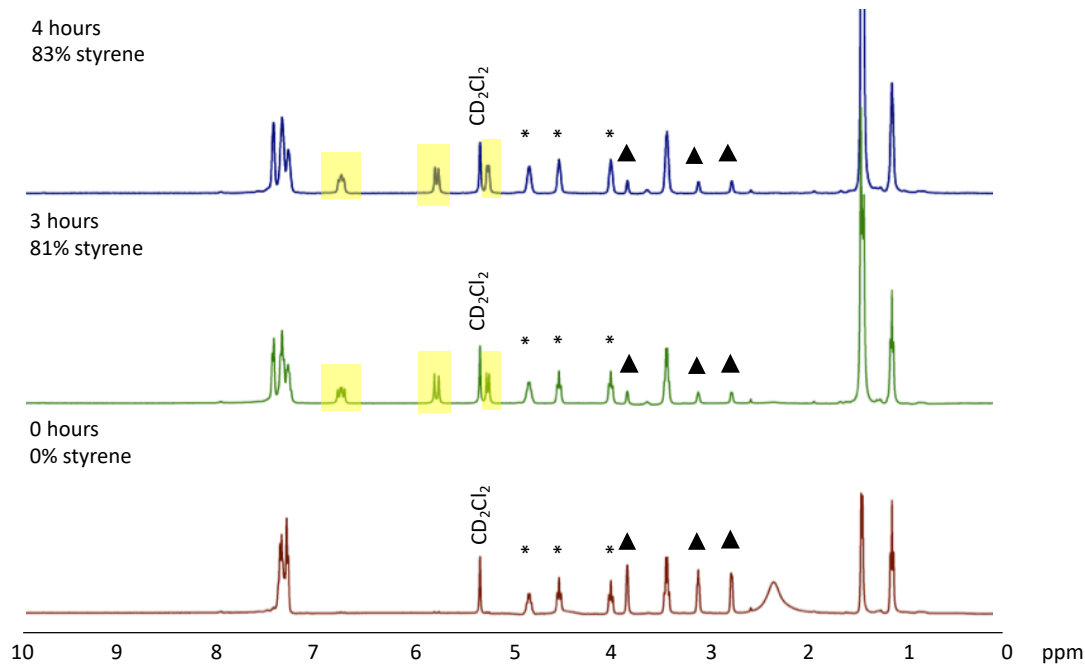


Figure S26. ^1H NMR spectra of the diamagnetic region of a crude reaction mixture of **4-OPMe₃** and styrene oxide (1 equiv) at 70 °C (CD_2Cl_2). Time points reveal loss of styrene oxide (black triangles) and growth of styrene (yellow highlight). Propylene carbonate (denoted by '*') was used as a ^1H NMR internal standard.

References:

1. C. Daniel and H. Hartl, *J. Am. Chem. Soc.*, 2005, **127**, 13978-13987.
2. B. E. Petel, W. W. Brennessel and E. M. Matson, *J. Am. Chem. Soc.*, 2018, **140**, 8424-8428.
3. B. E. Petel, A. A. Fertig, M. L. Maiola, W. W. Brennessel and E. M. Matson, *Inorg. Chem.*, 2019, *Advanced Article*, DOI: 10.1021/acs.inorgchem.9b00389.
4. M. N. Golovin, M. M. Rahman, J. E. Belmonte and W. P. Giering, *Organomet.*, 1985, **4**, 1981-1991.
5. C. A. Tolman, *Chem. Rev.*, 1977, **77**, 313-348.